

Language-Guided Visual Perception Disentanglement for Image Quality Assessment and Conditional Image Generation

Zhichao Yang¹ Leida Li^{1,2*} Pengfei Chen¹ Jinjian Wu¹ Giuseppe Valenzise³

¹Xidian University, ²Chongqing Three Gorges University, ³Paris-Saclay University

yangzhichao@stu.xidian.edu.cn, (ldli, chenpengfei, jinjian.wu)@xidian.edu.cn,

giuseppe.valenzise@l2s.centralesupelec.fr

Abstract

Contrastive vision-language models, such as CLIP, have demonstrated excellent zero-shot capability across semantic recognition tasks, mainly attributed to the training on a large-scale I&1T (one Image with one Text) dataset. This kind of multimodal representations often blend semantic and perceptual elements, placing a particular emphasis on semantics. However, this could be problematic for popular tasks like image quality assessment (IQA) and conditional image generation (CIG), which typically need to have fine control on perceptual and semantic features. Motivated by the above facts, this paper presents a new multimodal disentangled representation learning framework, which leverages disentangled text to guide image disentanglement. To this end, we first build an I&2T (one Image with a perceptual Text and a semantic Text) dataset, which consists of disentangled perceptual and semantic text descriptions for an image. Then, the disentangled text descriptions are utilized as supervisory signals to disentangle pure perceptual representations from CLIP’s original ‘coarse’ feature space, dubbed **DeCLIP**. Finally, the decoupled feature representations are used for both image quality assessment (technical quality and aesthetic quality) and conditional image generation. Extensive experiments and comparisons have demonstrated the advantages of the proposed method on the two popular tasks. The dataset, code, and model will be available.

1. Introduction

Semantics and perception are two basic perspectives for understanding an image. Compared to the concretization and objectivity of semantics, perception exhibits inherent abstraction and subjectivity [6, 33]. The learning of high-quality perceptual representations from images has been a longstanding research topic in the computer vision com-

*Corresponding author

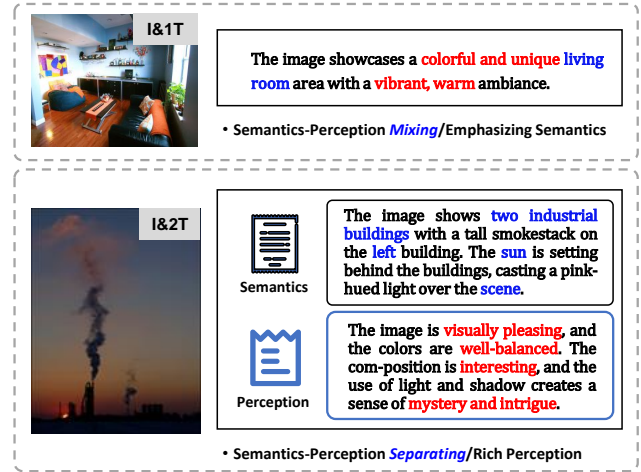


Figure 1. Conceptual difference between I&1T and I&2T. Upper: ‘I&1T’ features an image accompanied by one description that blends semantic and perceptual elements, with focus on semantics. Bottom: ‘I&2T’ features an image paired with two descriptions, offering rich perceptual insights while clearly differentiating between perception and semantics.

munity, with extensive applications including image recommendation [38, 56], image enhancement [32, 50], and style transfer [7, 23], etc.

In the past few years, significant efforts have been dedicated to the representation and extraction of perceptual features, encompassing aspects such as visual quality [18, 63, 68] and aesthetic appeal [19, 26, 43]. Early methodologies primarily relied on hand-crafted features, necessitating a substantial amount of domain expertise [5, 20]. In the deep learning era, Convolutional Neural Networks (CNNs) and Transformers have been commonly employed to uncover the perceptual representations embedded within large-scale datasets [13, 34]. However, such methods rely heavily on human perceptual annotations, typically in the form of Mean Opinion Score (MOS). Recent achievements in multimodal methods have integrated the language modality to

enhance the understanding of visual modality. The perceptual representation of the language modality has received considerable attention and investigation, significantly enhancing the perceptual understanding of the visual modality [19, 41].

Using image-text pairs with a cross-modal contrastive loss proves to be highly effective for multi-modal representation learning [60]. Contrastive Language-Image Pre-Training, i.e. CLIP [37], trained on a billion-level I&1T (one Image with one Text) dataset, demonstrates remarkable zero-shot generalization capability across a wide range of downstream tasks. However, this kind of text description typically mixes the semantic and perceptual aspects of an image, with more emphasis on semantics, as illustrated in the upper part of Fig. 1, which limits model’s perceptual representation capability. In this context, researchers have made significant effort in establishing datasets rich in perceptual descriptions [14, 52]. However, the entanglement between semantics and perception in the visual and language modalities remains challenging. This leads to significant limitations on the generalization capability of models in Image Quality Assessment (IQA) and multi-modal Conditional Image Generation (CIG). For IQA task, diversified semantic backgrounds poses a significant challenge to the evaluation capability of models, especially in cross-scene and cross-dataset contexts. For CIG task, the intricate coupling of semantics and perception within image prompts hinders generative models from obtaining accurate references, thereby affecting the final generation quality.

The perceptual description of an image, encompassing aspects such as clarity, light, composition etc., differs markedly from the corresponding semantic description, which pertains to scenes and objects, as illustrated in the bottom part of Fig. 1. Compared to the intricate entanglement between semantics and perception in the visual modality, the two aspects are relatively easy to differentiate in the language modality, which offers a natural form of decoupled supervision. Motivated by the above facts, this paper presents a novel multi-modal framework of Decoupled-Text Guided Image Disentangled Representation Learning for accurate vision-language alignment. First, we establish a dataset for multi-modal disentangled representation learning, called **I&2T** (one Image with a perceptual Text and a semantic Text), which features images with distinct perceptual and semantic descriptions. Concretely, we utilize existing multi-modal data with rich perceptual descriptions, leveraging the strong semantic understanding and summarization capabilities of Multi-modal Large Language Models (MLLMs, e.g., GeminiPro [9]) to design prompts for data generation. Building upon this, we explore the use of decoupled descriptions to refine CLIP’s original vision-language alignment space, dubbed **DeCLIP**. In particular, based on the original robust yet ‘coarse’ vision-language

space of CLIP, we leverage decoupled text descriptions as supervision to learn ‘pure’ perceptual and semantic representations of the visual modality. DeCLIP exhibits enhanced zero-shot generalization capability in image quality assessment, including technical quality and aesthetic quality. Moreover, we propose a method that enables nuanced control over the perceptual and semantic aspects of image generation by employing Decoupled vision Prompts to Adapt the vanilla Stable Diffusion [39], referred to as **DP-Adapter**.

We summarize the contributions of this work as follows:

- We present a new multi-modal framework of Decoupled-Text Guided Image Disentangled Representation Learning, referred to as DeCLIP, which can effectively disentangle the latent perceptual and semantic factors in pre-trained CLIP-like models, enabling more accurate and fine-grained vision-language alignment.
- We construct an I&2T dataset for multi-modal disentangled representation learning, which includes images accompanied by distinct perceptual and semantic descriptions. These decoupled descriptions provide supervision for the disentanglement of the visual modality.
- We utilize the decoupled alignment of vision-language representations from DeCLIP for two popular tasks: Image Quality Assessment and Conditional Image Generation. Extensive experiments and comparisons demonstrate that the model achieves excellent zero-shot generalization capability in both tasks.

2. Related Work

2.1. Image Quality Assessment

Image quality assessment aims to assess the subjective properties of images consistent with human perception [10], including technical quality [18, 42, 48, 62, 63, 68] and aesthetic quality [11, 19, 26, 27, 43, 57]. Early methods designed hand-crafted features to represent the perceptual characteristics of images, necessitating a substantial amount of domain expertise [44]. Recently, deep learning-based works focused on data-driven methods, which are typically based on large-scale datasets containing images and human ratings [13, 43]. More recently, the advancements in multi-modal vision have prompted researchers to focus on the perceptual description in the language modality [57, 63]. However, the intricate entanglement of semantics and perception in the visual modality remains a significant obstacle in enhancing the perceptual capabilities, leading to the inherent weakness in generalization of quality evaluation models. In this paper, we explore the use of decoupled text descriptions to disentangle pure perceptual representations from the visual modality, thereby enhancing the zero-shot generalization capability in image quality assessment.

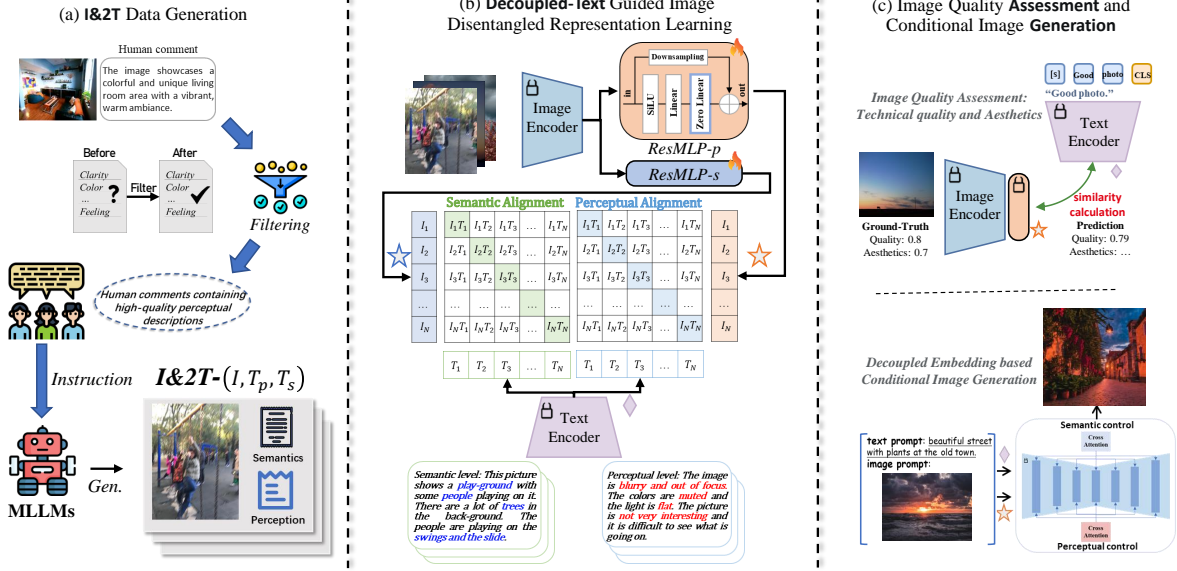


Figure 2. The overall framework of the proposed method. First, the I&T dataset, consisting of 112,769 image-text pairs formatted as (I, T_p, T_s) , is established. Building upon this, decoupled text is utilized as supervision to disentangle pure semantic and perceptual features. Finally, the resulting decoupled representations are employed for image quality assessment and conditional image generation.

2.2. Multi-modal Conditional Image Generation

Recent advancements in multi-modal conditional image generation often leverage pre-trained vision-language models like CLIP [37], alongside large diffusion models like Stable Diffusion [39]. CLIP bridges the gap between vision and language, while Stable Diffusion functions as a latent diffusion model trained on a vast dataset. IP-Adapter [58] utilized a decoupled cross-attention mechanism to connect CLIP with pretrained text-to-image diffusion models, enabling image prompt capability. However, achieving accurate control over the semantic and perceptual aspects of generated images is extremely challenging with CLIP’s coarse alignment space. To address this issue, this paper presents the decoupled vision-language representations as prompts to enhance conditional image generation.

2.3. Disentangled Representation Learning

Disentangled representation learning aims to isolate intrinsic latent factors within data, transforming them into distinct and controllable representations [49]. In the context of single modality, some studies utilized image augmentation techniques to separate content variables from the latent space by inducing significant perceptual changes [46, 64]. For multi-modal scenarios, CLAP [1] employed text augmentation with a cross-modal contrastive loss to disentangle latent content variables. In contrast to these approaches, the proposed method utilizes decoupled semantic and perceptual descriptions to disentangle visual modality.

3. Proposed Method

In this section, we provide a detailed introduction to the proposed approach. The pipeline is illustrated in Fig. 2. First, the I&T dataset, consisting of images paired with distinct perceptual and semantic descriptions, is established. Building upon this, the decoupled text is utilized as supervision to disentangle pure perceptual and semantic features from the visual modality. Finally, the disentangled visual representations are employed for image quality assessment and conditional image generation.

Data Source	Filtered Quantity	Image Types
AesExpert [14]	21390	Natural, Art, AIGC
Q-Instruct [52]	11753	Natural, AIGC
ShareGPT4v [2]	22643	Natural, Art
AVA-Comments [67]	56983	Natural
I&T	112,769	Natural, Art, AIGC

Table 1. Overview of the data source for I&T. The filtered quantity and image types are also presented.

3.1. I&T Data Generation

Compared to the intricate entanglement of semantics and perception in the visual modality, the language modality is inherently easier to disentangle [4]. Words that describe semantics are frequently linked to objects or scenes, whereas words that pertain to perception are often associated with attributes, such as clarity, composition, and emotional res-

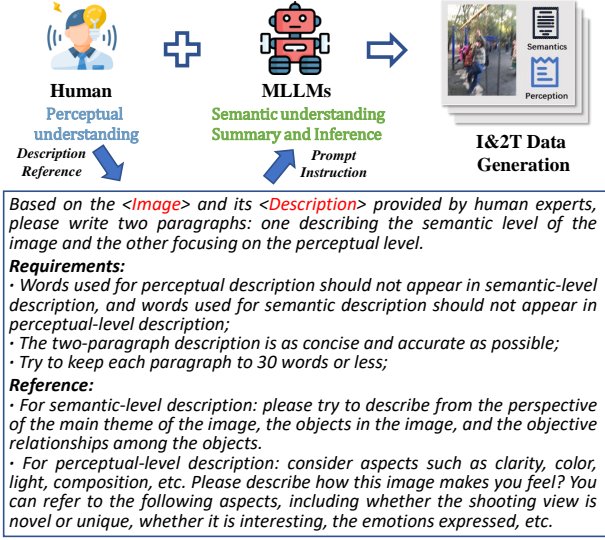


Figure 3. The I&2T database construction pipeline and the prompt design. The perceptual abilities of humans, in conjunction with the semantic understanding and reasoning capabilities of MLLMs, collaboratively contribute to data generation.

onance. Recently, Zhong *et al.* [65] conducted a manual selection of object-related and aesthetics-related words to compute the Aesthetic Relevance Score (ARS) for sentences. Yang *et al.* [57] employed semantic-related and attribute-related tags to extract corresponding features for evaluating image aesthetics. Inspired by these works, we construct the I&2T dataset, which features images with distinct perceptual and semantic descriptions.

First, we select representative perception-related multi-modal dataset (e.g., AVA-Comments [67]), as well as datasets used for training perceptual MLLMs (e.g., Q-Instruct [52], AesExpert [14], ShareGPT4v [2]), to serve as data sources. These datasets contain rich human-generated perceptual descriptions, but the quality varies significantly. Therefore, we employ the library rich in perceptual vocabulary [57] to filter these datasets. The number of perceptual vocabularies included in each description serves as selection criterion. We exclude data containing fewer than seven perceptual vocabulary items, which is considered as low-quality perceptual description. Finally, we collect 112,769 image-text pairs as the initial data, including natural, art and AIGC types, as illustrated in Tab. 1.

Compared to perceptual understanding, the semantic understanding of general Multi-modal Large Language Models (MLLMs) is more reliable [15, 51]. Consequently, we employ high-quality human-generated perceptual descriptions as instructions to craft prompts that facilitate the MLLMs in re-labeling decoupled semantic and perceptual descriptions for each image. Concretely, we formulate specific descriptive requirements and references to guide

MLLMs in generating decoupled descriptions. The complete prompt and the construction pipeline are illustrated in Fig. 3.

The final I&2T dataset can be represented as follows:

$$\mathcal{D}_{I\&2T} = \{(I^i, T_p^i, T_s^i)\}_{i=1}^N, \quad (1)$$

where I^i denotes the i -th image, (T_p^i, T_s^i) denotes the corresponding perceptual and semantic descriptions, and N represents the number of images.

3.2. Decoupled-Text Guided Image Disentangled Representation Learning

Building upon the I&2T dataset, we utilize decoupled textual descriptions as supervision to refine vision-language alignment of CLIP, thereby achieving disentangled perceptual and semantic representations in the visual modality, dubbed as DeCLIP.

Preliminary of CLIP: CLIP is a Contrastive Language-Image Pretraining model that establishes a joint embedding space for images and texts. It consists of an image encoder and a text encoder, trained using a contrastive learning framework on a large-scale I&1T dataset.

Encoding Image: Compared to the strong semantic alignment capabilities, CLIP’s perceptual abilities are relatively weaker. However, previous studies [12] and [48] have demonstrated the potential of CLIP in evaluating both aesthetics and technical quality of images. Furthermore, many low-level visual tasks, such as image restoration [53] and image enhancement [29], have utilized CLIP’s perceptual understanding. These investigations highlight the substantial perceptual understanding potential within CLIP’s latent alignment space. Consequently, we introduce two simple but effective projectors on top of the existing image encoder in CLIP for disentanglement: $ResMLP_p$ and $ResMLP_s$ [1], which consist of a residual block featuring a zero-initialized, bias-free linear layer. The zero-linear components learn specific knowledge for perceptual alignment and semantic alignment respectively, while the residual connection enables learning directly from the CLIP’s pre-trained representation space, avoiding a random starting point. Specifically, the i -th image from the I&2T dataset, is mapped to two embedding spaces, as follows:

$$\mathbf{f}_I^i = E_I(I^i), \quad (2)$$

$$\mathbf{f}_{I(p)}^i = ResMLP_p(\mathbf{f}_I^i), \mathbf{f}_{I(s)}^i = ResMLP_s(\mathbf{f}_I^i), \quad (3)$$

where $\mathbf{f}_{I(p)}^i, \mathbf{f}_{I(s)}^i$ represent mapped visual embeddings corresponding to perception and semantics, respectively.

Encoding Text: Considering the differences in terminology and focus between semantic and perceptual descriptions, we directly employ CLIP’s text encoder E_T to obtain distinct textual representations. Concretely, the perceptual

and semantic texts corresponding to the i -th image, are inputted to generate decoupled embeddings:

$$\mathbf{f}_{T(p)}^i = E_T(T_p^i), \mathbf{f}_{T(s)}^i = E_T(T_s^i), \quad (4)$$

where $\mathbf{f}_{T(p)}^i, \mathbf{f}_{T(s)}^i$ denote textual embeddings associated with perception and semantics, respectively.

Disentangled Representation Learning: Based on CLIP’s original joint embedding space for images and texts, we leverage the decoupled texts of the I&2T dataset to achieve decoupled vision-language alignment. Specifically, we align the decoupled perceptual and semantic textual embeddings with their corresponding visual representations. This transforms the original unified alignment space into two distinct spaces: one for perceptual alignment and the other for semantic alignment. This process is achieved through two cross-modal contrastive losses:

$$\mathcal{L}^{Con} = \mathcal{L}_p^{Con} + \mathcal{L}_s^{Con}, \quad (5)$$

$$\mathcal{L}_p^{Con} = -\frac{1}{B} \sum_i \log \frac{\exp(\mathbf{f}_{I(p)}^i \cdot \mathbf{f}_{T(p)}^i / \tau)}{\sum_{j=1}^B \exp(\mathbf{f}_{I(p)}^i \cdot \mathbf{f}_{T(p)}^j / \tau)}, \quad (6)$$

$$\mathcal{L}_s^{Con} = -\frac{1}{B} \sum_i \log \frac{\exp(\mathbf{f}_{I(s)}^i \cdot \mathbf{f}_{T(s)}^i / \tau)}{\sum_{j=1}^B \exp(\mathbf{f}_{I(s)}^i \cdot \mathbf{f}_{T(s)}^j / \tau)}, \quad (7)$$

where \mathcal{L}_p^{Con} is the image-to-perception contrastive loss, \mathcal{L}_s^{Con} is the image-to-semantics contrastive loss, τ is the temperature coefficient, (\cdot) denotes the inner product operation, and B is the batch size. It is essential to note that optimization is confined solely to the parameters of the two *ResMLP* modules.

3.3. Image Quality Assessment and Conditional Image Generation

In this section, we utilize the decoupled vision-language features of DeCLIP for both Image Quality Assessment and Conditional Image Generation tasks.

Image Quality Assessment: Compared to I&1T, the I&2T dataset offers rich perceptual descriptions that encompass various aspects, including visual quality and aesthetic appeal. To validate the effectiveness of the decoupled perceptual representations of images, we adopt a straightforward approach by evaluating DeCLIP’s zero-shot capability across two popular perceptual quality evaluation tasks: Image Technical Quality Assessment (TQA) and Image Aesthetics Quality Assessment (AQA).

For TQA and AQA, we utilize the decoupled perceptual visual features in conjunction with antonym prompts (e.g., ‘Good photo.’ and ‘Bad photo.’) to predict image quality/aesthetics scores [48]. Softmax function and cosine sim-

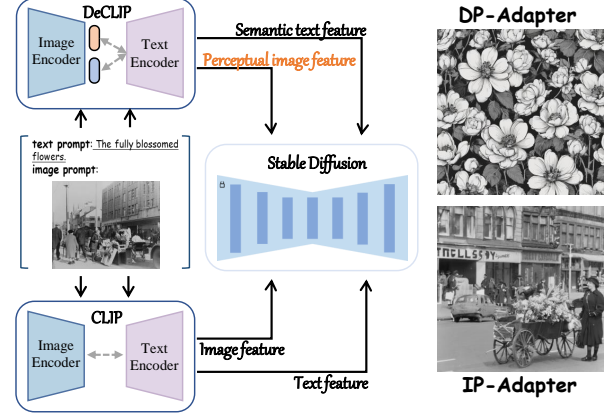


Figure 4. DP-Adapter vs. IP-Adapter. The former utilizes the decoupled vision-language representations obtained from DeCLIP to control Stable Diffusion, while the latter directly employs CLIP’s vision-language representations for generative control.

ilarity are employed to implement this process:

$$\bar{s} = \frac{e^{\cos(\mathbf{f}_{I(p)}, \mathbf{f}_{TP})}}{e^{\cos(\mathbf{f}_{I(p)}, \mathbf{f}_{TP})} + e^{\cos(\mathbf{f}_{I(p)}, \mathbf{f}_{TN})}}, \quad (8)$$

where \bar{s} denotes the predicted score, $\cos(\cdot)$ is the cosine similarity function, and $\mathbf{f}_{TP}, \mathbf{f}_{TN}$ represent the positive and negative textual features of antonym prompts.

Conditional Image Generation: The image-text alignment capabilities of CLIP have been commonly applied in the realm of conditional image generation. IP-Adapter [58] presents a decoupled cross-attention mechanism based on CLIP for multi-modal conditional image generation. The training process can be expressed as:

$$\mathcal{L} = \mathbb{E}_{x_0, \epsilon, c, t} \|\epsilon - \epsilon_{\theta(x_t, c, t)}\|^2, \quad (9)$$

where, a denoising process generates samples from Gaussian noise $x_t \sim N(0, 1)$ with a trained denoising model $\epsilon_{\theta(x_t, c, t)}$ parameterized by θ . The c represents the condition, which is generated by the text embeddings \mathbf{f}_T and image embeddings \mathbf{f}_I from CLIP, and integrated into the Stable Diffusion through the decoupled cross-attention module.

CLIP empowers the Stable Diffusion with the capability for multi-modal conditional image generation. Nevertheless, significant conflicts in prompts, such as overt semantic discrepancies, can adversely impact the quality of generated outputs, as illustrated at the bottom of Fig. 4. The decoupling of vision-language alignment spaces provides a viable solution to this challenge. By partitioning the original alignment space of CLIP into distinct perceptual and semantic sub-spaces, we can achieve flexible and more accurate control over the respective aspects of the generated images.

Quality	Dist Type	Synthetic								Authentic						AIGC	
	Databases	LIVE		CSIQ		TID2013		KADID		LIVEC		KonIQ		SPAQ		AGIQA-3K	
	Metrics	SRCC	PLCC	SRCC	PLCC	SRCC	PLCC	SRCC	PLCC	SRCC	PLCC	SRCC	PLCC	SRCC	PLCC	SRCC	PLCC
	CLIP	0.510	0.537	0.504	0.558	0.450	0.497	0.387	0.392	0.355	0.318	0.327	0.352	0.439	0.381	0.308	0.359
DeCLIP		0.725	0.707	0.569	0.621	0.551	0.594	0.502	0.527	0.624	0.513	0.602	0.593	0.793	0.446	0.387	0.447
	(↑%)	↑21.5	↑17.0	↑6.5	↑6.3	↑10.1	↑9.7	↑11.5	↑13.5	↑26.9	↑19.5	↑27.5	↑24.1	↑35.4	↑6.5	↑7.9	↑8.8
Aesthetics	Img Type	Natural								Artistic				AIGC			
	Databases	AVA		AADB		PARA		EVA		BAID		APDD		RichHF-18K		SAC	
	Metrics	SRCC	PLCC	SRCC	PLCC	SRCC	PLCC	SRCC	PLCC	SRCC	PLCC	SRCC	PLCC	SRCC	PLCC	SRCC	PLCC
	CLIP	0.387	0.403	0.334	0.336	0.548	0.550	0.465	0.464	0.109	0.084	0.319	0.320	-0.078	-0.057	0.241	0.252
DeCLIP		0.395	0.409	0.403	0.401	0.627	0.605	0.506	0.516	0.171	0.148	0.411	0.388	-0.018	-0.036	0.254	0.264
	(↑%)	↑0.8	↑0.6	↑6.9	↑6.5	↑7.9	↑5.5	↑4.1	↑5.2	↑6.2	↑6.4	↑9.2	↑6.8	↑6.0	↑2.1	↑1.3	↑1.2

Table 2. Comparison between the proposed DeCLIP and the vanilla CLIP (Zero-shot) across two perceptual quality evaluation tasks: Technical Quality and Aesthetics. The relative improvements are displayed.

In particular, we utilize the decoupled vision-language representations of DeCLIP to adapt the Stable Diffusion for image generation. This enables flexible control over the perceptual and semantic aspects of generated images through the complementary use of image and text:

$$c \in \{(\mathbf{f}_{I(p)}, \mathbf{f}_{T(s)}), (\mathbf{f}_{I(s)}, \mathbf{f}_{T(p)})\}, \quad (10)$$

where $(\mathbf{f}_{I(p)}, \mathbf{f}_{T(s)})$ and $(\mathbf{f}_{I(s)}, \mathbf{f}_{T(p)})$ represent two distinct control types: ‘perceptual image + semantic text’ and ‘semantic image + perceptual text’, respectively. An example is illustrated in the upper part of Fig. 4. These two modes better meet users’ practical application needs, such as a user integrating perceptual elements from an aesthetically pleasing image into their desired semantic content for generation. It is worth noting that we do not retrain the Stable Diffusion and Attention module, because DeCLIP and CLIP essentially belong to the same alignment space.

4. Experiment

4.1. Implementation Details

We utilize ViT version of CLIP as the foundational model for disentangled representation learning. It is important to note that we only introduce two projectors during training, while maintaining all original settings of CLIP, including a fixed input size (e.g., 224×224) and the original parameters. The projector comprises two linear layers and a SiLU activation function, with a latent dimension set to 1024. Data augmentation during training involves random cropping. For disentangled learning on the I&2T dataset, we train with a batch size of 1024 for 200 epochs, employing a learning rate of 1e-5 along with a weight decay of 5e-2. The temperature coefficient τ is set to 0.07. All experiments are conducted using the AdamW [31] optimizer with four

NVIDIA GeForce RTX 3090 GPUs.

4.2. Performance on Image Quality Assessment

Datasets and Metrics: To evaluate the efficacy of the decoupled perceptual representations, we conduct experiments on two representative perceptual quality evaluation tasks: image technical quality assessment and image aesthetic quality assessment. For TQA, we test datasets with three different types of distortions, including synthetic distortions (LIVE [40], CSIQ [22], TID2013 [35], KADID [30]), real-world distortions (LIVEC [8], KonIQ [13], SPAQ [6]), and AI-generated distortions (AGIQA-3K [24]). In terms of AQA, we test datasets with three distinct types of images: natural images (AVA [34], AADB [21], PARA [55], EVA [17]), artistic images (BAID [59], APDD [16]), and AIGC images (RichHF-18K [28], SAC [36]). We employ the Spearman Rank Correlation Coefficient (SRCC) and Pearson Linear Correlation Coefficient (PLCC) to measure model performance.

Zero-Shot Performance: We first utilize DeCLIP’s vision-language alignment capability in the decoupled perceptual space for zero-shot evaluation, and compare it with the vanilla CLIP. The results are summarized in Tab. 2. It is observed that DeCLIP significantly outperforms CLIP across all two perceptual quality evaluation tasks. Notably, for the TQA task, DeCLIP demonstrates a more pronounced improvement on authentic distortions compared to synthetic and AI-generated. In addition, DeCLIP exhibits more significant advantage when applied to natural images.

Generalization Performance: The intricate entanglement of semantics and perception poses significant challenge to the generalization ability of perceptual quality evaluation models. To evaluate the generalization of DeCLIP on perceptual evaluation, we conduct cross-database exper-

Training	KonIQ-10k		
Testing	SPAQ	AGIQA	KADID
DBCNN [62]	0.806	0.641	0.484
MetaIQA [68]	0.841	0.552	0.554
HyperIQA [42]	0.788	0.640	0.468
MUSIQ [18]	0.863	0.630	0.556
CLIP-IQA [48]	0.864	0.685	0.654
LIQE [63]	0.833	0.708	0.662
DeCLIP	0.867	0.711	0.741

Training	AVA		
Testing	AADB	PARA	APDD
NIMA [43]	0.471	0.626	0.220
PA-IAA [26]	0.527	0.655	0.428
TANet [11]	0.328	0.471	0.351
TAVAR [27]	0.480	0.652	0.413
VILA [19]	0.548	0.649	0.426
TMCR [57]	0.507	0.622	0.483
DeCLIP	0.583	0.669	0.549

Table 3. Comparison of cross-dataset performance on technical and aesthetic quality assessment. The SRCC index is reported. Bolded numbers indicate the best performance.

iment. We compare DeCLIP with state-of-the-art models in technical quality and aesthetic quality assessments. We utilize CoOP [66] to train a textual prompt vector for the parameter-frozen DeCLIP, enabling cross-database testing. The experimental results are listed in Tab. 3. The results demonstrate that DeCLIP achieves the best performance. Notably, DeCLIP demonstrates a significant advantage in the TQA tests from real distortion (KonIQ-10k) to synthetic distortion (KADID), as well as in the AQA tests transitioning from natural images (AVA) to artistic images (APDD). This further validates the effectiveness of decoupled perceptual representations.

Fine-Grained Attribute Prediction: In addition to the overall perception of an image, we also evaluate the zero-shot performance of DeCLIP on predicting fine-grained attributes. Specifically, we conduct experiments on two databases, SPAQ [6] and PARA [55], which provide annotations for various attributes, including quality attributes such as noise and contrast, as well as aesthetic attributes like composition and depth-of-field. The results are summarized in Tab. 4. It is observed from the table that DeCLIP outperforms CLIP significantly in various quality and aesthetic attributes. Particularly, DeCLIP demonstrates an approximate 20% improvement over CLIP for the quality attributes of colorfulness, contrast, and noise. Similarly, DeCLIP exhibits a significant advantage for aesthetic attributes of depth-of-field and light. These results further demonstrate the superiority of DeCLIP on understanding fine-grained at-

TQA Attribute (SPAQ database)				AQA Attribute (PARA database)			
Attribute	Model	SRCC	PLCC	Attribute	Model	SRCC	PLCC
Brightness	CLIP	0.439	0.437	Composition	CLIP	0.274	0.326
	DeCLIP	0.584	0.529		DeCLIP	0.369	0.431
Colorfulness	CLIP	0.278	0.251	Color	CLIP	0.444	0.471
	DeCLIP	0.576	0.412		DeCLIP	0.530	0.563
Contrast	CLIP	-0.135	-0.154	Depth-of-Field	CLIP	0.113	0.172
	DeCLIP	0.311	0.239		DeCLIP	0.374	0.445
Noise	CLIP	0.195	0.112	Light	CLIP	0.488	0.536
	DeCLIP	0.573	0.286		DeCLIP	0.591	0.622
Sharpness	CLIP	0.638	0.395	Object emphasis	CLIP	0.259	0.281
	DeCLIP	0.794	0.256		DeCLIP	0.325	0.317

Table 4. Performance comparison on attribute prediction (zero-shot). Bolded numbers indicate better performance.

tributes, which could be highly desired in evaluation interpretability.

4.3. Performance on Conditional Image Generation

The decoupled perceptual and semantic vision-language alignment sub-spaces of DeCLIP provide a flexible control foundation for image generation tasks. Specifically, the decoupled visual features, in conjunction with complementary semantic or perceptual text descriptions, can serve as accurate prompts to guide the corresponding aspects of generated images. To demonstrate the capability of DP-Adapter in controlling the semantic and perceptual aspects in image generation, we conduct qualitative and quantitative comparisons with the state-of-the-art multi-modal generative models, including IP-Adapter [58], Versatile Diffusion [54], ControlNet Shuffle [61], BLIP-Diffusion [25], and InstantStyle [47].

Qualitative Results: Fig. 5 shows a qualitative comparison between our proposed DP-Adapter and five popular multi-modal generative models. We compare the generative performance of all models under two different control types, using identical image and text prompts.

Perceptual Image + Semantic Text signifies that the image prompt provides perceptual reference, while the text prompt offers semantic reference for image generation. As illustrated in the top two rows in Fig. 5, DP-Adapter demonstrates superior generative performance compared to the other models. The compared models exhibit varying degrees of ‘mismatch’ defects. Notably, ControlNet Shuffle and InstantStyle do not incorporate semantic elements from the text prompt such as ‘street’ and ‘lamp’. Versatile Diffusion exhibits a significant perceptual discrepancy with the image prompt. The substantial semantic differences between image and text prompts severely impact generative outcomes. In contrast, DP-Adapter effectively mitigates this issue by utilizing decoupled representations.

Semantic Image + Perceptual Text indicates that the image prompt provides semantic reference, while the

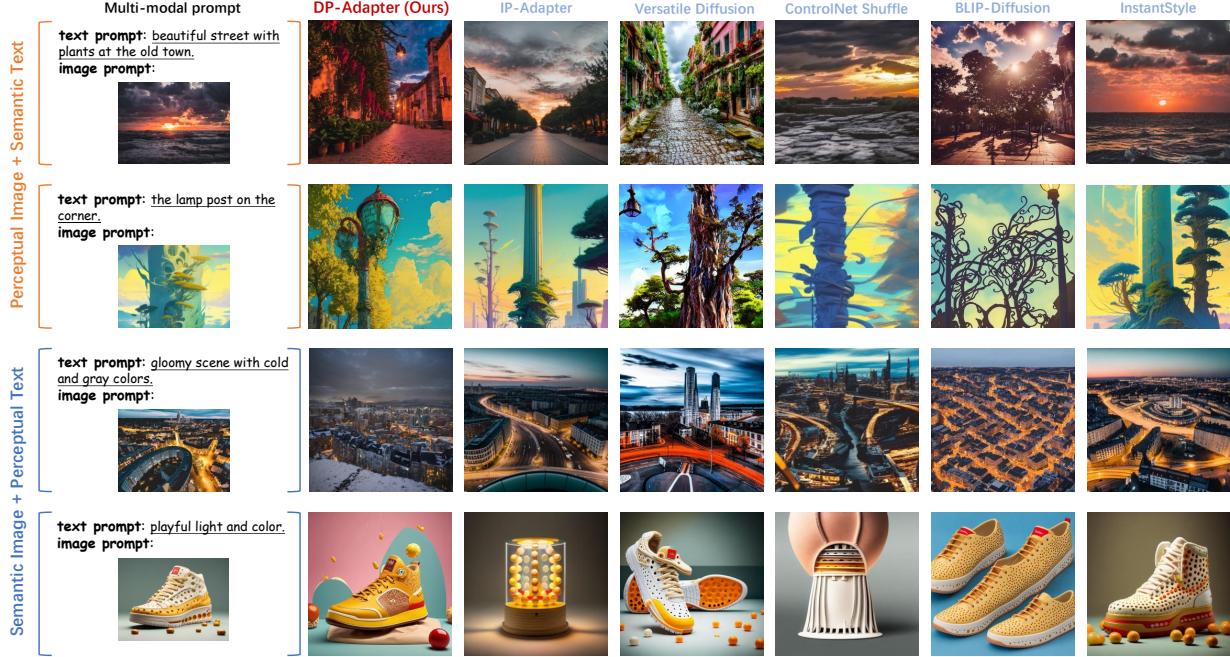


Figure 5. The visual comparison of the DP-Adapter with other methods conditioned on different perceptual and semantic prompts.

text prompt provides perceptual reference for generating images. Similarly, from the examples in the bottom two rows of Fig. 5, we observe that DP-Adapter also yields the best generation results. An interesting finding is that the word ‘light’ has different interpretations from semantic and perceptual perspectives. Both IP-Adapter and ControlNet Shuffle interpret it as a semantic element, which significantly deviates from the intended control objectives. These results demonstrate the advantage of DP-Adapter in controlling both perceptual and semantic aspects in image generation.

Quantitative Results: We further conduct a user study to evaluate the semantic and perceptual control capabilities of DP-Adapter. Specifically, we collected 100 pairs of image-text as conditions for image generation. The images are sourced from existing datasets [45], including natural, artistic, and AIGC. The textual descriptions are categorized into two types: perception and semantics. Some of the descriptions originate from established datasets (e.g., COCO Captions [3]), while others are generated by Large Language Model. These text prompts are then randomly combined with the selected image prompts to produce 100 image-text pairs, which are then used for image generation with DP-Adapter and the compared models.

We recruited ten volunteers to perform the user study. Specifically, they are asked to score (1-5) the generated images from three dimensions: Semantic Consistency (SC), Perceptual Consistency (PC), and Overall Feeling (OF). The first two are used to assess the alignment between the

Metrics	CC	OF
IP-Adapter [58]	0.628	0.536
Versatile Diffusion [54]	0.521	0.400
ControlNet Shuffle [61]	0.465	0.293
BLIP-Diffusion [25]	0.436	0.292
InstantStyle [47]	0.464	0.288
DP-Adapter	0.696	0.641

Table 5. Quantitative comparisons from human on generative performance. Best result is marked in bold.

generated images and the corresponding semantic (e.g., objects) and perceptual (e.g., color) conditions. For OF, factors such as adherence to conditions, presence of defects, and aesthetic appeal are considered. Finally, we calculate the average score for each dimension and derive an overall Condition Consistency (CC) by averaging SC and PC scores, to assess the generative performance. The results are summarized in Tab. 5. The CC and OF metrics indicate that the proposed DP-Adapter achieves the highest generation quality. This is attributed to the decoupled vision-language representations.

5. Conclusion

In this paper, we propose a new multi-modal framework for disentangled representation learning. Our method leverages MLLMs-assisted text disentanglement to learn perception-specific and semantics-specific visual repre-

sentations, thereby achieving fine-grained vision-language alignment. Comprehensive experiments conducted on both image quality assessment and conditional image generation tasks demonstrate the remarkable zero-shot generalization capability of these representations. While very encouraging results have been achieved in this work, the decoupled features still hold significant potential for further enhancement and application, especially in perception-related tasks like image enhancement and restoration.

References

- [1] Yichao Cai, Yuhang Liu, Zhen Zhang, and Javen Qinfeng Shi. Clap: Isolating content from style through contrastive learning with augmented prompts. In *Eur. Conf. Comput. Vis.*, 2024. 3, 4
- [2] Lin Chen, Jinsong Li, Xiaoyi Dong, Pan Zhang, Conghui He, Jiaqi Wang, Feng Zhao, and Dahua Lin. Sharegpt4v: Improving large multi-modal models with better captions. *arXiv preprint arXiv:2311.12793*, 2023. 3, 4
- [3] Xinlei Chen, Hao Fang, Tsung-Yi Lin, Ramakrishna Vedantam, Saurabh Gupta, Piotr Dollár, and C Lawrence Zitnick. Microsoft coco captions: Data collection and evaluation server. *arXiv preprint arXiv:1504.00325*, 2015. 8
- [4] De Cheng, Zhipeng Xu, Xinyang Jiang, Nannan Wang, Dongsheng Li, and Xinbo Gao. Disentangled prompt representation for domain generalization. In *IEEE Conf. Comput. Vis. Pattern Recog.*, pages 23595–23604, 2024. 3
- [5] Ritendra Datta, Dhiraj Joshi, Jia Li, and James Z Wang. Studying aesthetics in photographic images using a computational approach. In *Eur. Conf. Comput. Vis.*, pages 288–301, 2006. 1
- [6] Yuming Fang, Hanwei Zhu, Yan Zeng, Kede Ma, and Zhou Wang. Perceptual quality assessment of smartphone photography. In *IEEE Conf. Comput. Vis. Pattern Recog.*, pages 3677–3686, 2020. 1, 6, 7
- [7] Leon A Gatys, Alexander S Ecker, Matthias Bethge, Aaron Hertzmann, and Eli Shechtman. Controlling perceptual factors in neural style transfer. In *IEEE Conf. Comput. Vis. Pattern Recog.*, pages 3985–3993, 2017. 1
- [8] Deepti Ghadiyaram and Alan C Bovik. Massive online crowdsourced study of subjective and objective picture quality. *IEEE Trans. Image Process.*, 25(1):372–387, 2015. 6
- [9] Google. Build with gemini, 2023. 2
- [10] Henrik Hagtvedt, Vanessa M Patrick, and Reidar Hagtvedt. The perception and evaluation of visual art. *Empirical studies of the arts*, 26(2):197–218, 2008. 2
- [11] Shuai He, Yongchang Zhang, Rui Xie, Dongxiang Jiang, and Anlong Ming. Rethinking image aesthetics assessment: Models, datasets and benchmarks. In *Proc. AAAI Conf. Artif. Intell.*, pages 942–948, 2022. 2, 7
- [12] Simon Hentschel, Konstantin Kobs, and Andreas Hotho. Clip knows image aesthetics. *Frontiers in Artificial Intelligence*, 5:976235, 2022. 4
- [13] Vlad Hosu, Hanhe Lin, Tamas Sziranyi, and Dietmar Saupe. Koniq-10k: An ecologically valid database for deep learning of blind image quality assessment. *IEEE Trans. Image Process.*, 29:4041–4056, 2020. 1, 2, 6
- [14] Yipo Huang, Xiangfei Sheng, Zhichao Yang, Quan Yuan, Zhichao Duan, Pengfei Chen, Leida Li, Weisi Lin, and Guangming Shi. Aesexpert: Towards multi-modality foundation model for image aesthetics perception. In *ACM Int. Conf. Multimedia*, pages 5911–5920, 2024. 2, 3, 4
- [15] Yipo Huang, Quan Yuan, Xiangfei Sheng, Zhichao Yang, Haoning Wu, Pengfei Chen, Yuzhe Yang, Leida Li, and Weisi Lin. Aesbench: An expert benchmark for multimodal large language models on image aesthetics perception. *arXiv preprint arXiv:2401.08276*, 2024. 4
- [16] Xin Jin, Qianqian Qiao, Yi Lu, Shan Gao, Heng Huang, and Guangdong Li. Paintings and drawings aesthetics assessment with rich attributes for various artistic categories. In *Proc. AAAI Conf. Artif. Intell.*, 2024. 6
- [17] Chen Kang, Giuseppe Valenzise, and Frédéric Dufaux. Eva: An explainable visual aesthetics dataset. In *Joint workshop on aesthetic and technical quality assessment of multimedia and media analytics for societal trends*, pages 5–13, 2020. 6
- [18] Junjie Ke, Qifei Wang, Yilin Wang, Peyman Milanfar, and Feng Yang. Musiq: Multi-scale image quality transformer. In *IEEE Conf. Comput. Vis. Pattern Recog.*, pages 5148–5157, 2021. 1, 2, 7
- [19] Junjie Ke, Keren Ye, Jiahui Yu, Yonghui Wu, Peyman Milanfar, and Feng Yang. Vila: Learning image aesthetics from user comments with vision-language pretraining. In *IEEE Conf. Comput. Vis. Pattern Recog.*, pages 10041–10051, 2023. 1, 2, 7
- [20] Yan Ke, Xiaou Tang, and Feng Jing. The design of high-level features for photo quality assessment. In *IEEE Conf. Comput. Vis. Pattern Recog.*, pages 419–426. IEEE, 2006. 1
- [21] Shu Kong, Xiaohui Shen, Zhe Lin, Radomir Mech, and Charles Fowlkes. Photo aesthetics ranking network with attributes and content adaptation. In *Eur. Conf. Comput. Vis.*, pages 662–679, 2016. 6
- [22] Eric C Larson and Damon M Chandler. Most apparent distortion: full-reference image quality assessment and the role of strategy. *Journal of electronic imaging*, 19(1):011006–011006, 2010. 6
- [23] Hsin-Ying Lee, Hung-Yu Tseng, Jia-Bin Huang, Maneesh Singh, and Ming-Hsuan Yang. Diverse image-to-image translation via disentangled representations. In *Eur. Conf. Comput. Vis.*, pages 35–51, 2018. 1
- [24] Chunyi Li, Zicheng Zhang, Haoning Wu, Wei Sun, Xiongkuo Min, Xiaohong Liu, Guangtao Zhai, and Weisi Lin. Agiqa-3k: An open database for ai-generated image quality assessment. *IEEE Trans. Circuit Syst. Video Technol.*, 2023. 6
- [25] Dongxu Li, Junnan Li, and Steven Hoi. Blip-diffusion: Pre-trained subject representation for controllable text-to-image generation and editing. *Adv. Neural Inform. Process. Syst.*, 36, 2024. 7, 8
- [26] Leida Li, Hancheng Zhu, Sicheng Zhao, Guiguang Ding, and Weisi Lin. Personality-assisted multi-task learning for generic and personalized image aesthetics assessment. *IEEE Trans. Image Process.*, 29:3898–3910, 2020. 1, 2, 7

- [27] Leida Li, Yipo Huang, Jinjian Wu, Yuzhe Yang, Yaqian Li, Yandong Guo, and Guangming Shi. Theme-aware visual attribute reasoning for image aesthetics assessment. *IEEE Trans. Circuit Syst. Video Technol.*, 33(9):4798–4811, 2023. 2, 7
- [28] Youwei Liang, Junfeng He, Gang Li, Peizhao Li, Arseniy Klimovskiy, Nicholas Carolan, Jiao Sun, Jordi Pont-Tuset, Sarah Young, Feng Yang, et al. Rich human feedback for text-to-image generation. In *IEEE Conf. Comput. Vis. Pattern Recog.*, pages 19401–19411, 2024. 6
- [29] Zhixin Liang, Chongyi Li, Shangchen Zhou, Ruicheng Feng, and Chen Change Loy. Iterative prompt learning for unsupervised backlit image enhancement. In *Int. Conf. Comput. Vis.*, pages 8094–8103, 2023. 4
- [30] Hanhe Lin, Vlad Hosu, and Dietmar Saupe. Kadid-10k: A large-scale artificially distorted iqa database. In *2019 Eleventh International Conference on Quality of Multimedia Experience (QoMEX)*, pages 1–3. IEEE, 2019. 6
- [31] I Loshchilov. Decoupled weight decay regularization. *arXiv preprint arXiv:1711.05101*, 2017. 6
- [32] Boyu Lu, Jun-Cheng Chen, and Rama Chellappa. Unsupervised domain-specific deblurring via disentangled representations. In *IEEE Conf. Comput. Vis. Pattern Recog.*, pages 10225–10234, 2019. 1
- [33] Xin Lu, Zhe Lin, Xiaohui Shen, Radomir Mech, and James Z Wang. Deep multi-patch aggregation network for image style, aesthetics, and quality estimation. In *Int. Conf. Comput. Vis.*, pages 990–998, 2015. 1
- [34] Naila Murray, Luca Marchesotti, and Florent Perronnin. Ava: A large-scale database for aesthetic visual analysis. In *IEEE Conf. Comput. Vis. Pattern Recog.*, pages 2408–2415. IEEE, 2012. 1, 6
- [35] Nikolay Ponomarenko, Lina Jin, Oleg Ieremeiev, Vladimir Lukin, Karen Egiazarian, Jaakko Astola, Benoit Vozel, Kacem Chehdi, Marco Carli, Federica Battisti, et al. Image database tid2013: Peculiarities, results and perspectives. *Signal processing: Image communication*, 30:57–77, 2015. 6
- [36] John David Pressman, Katherine Crowson, and Simulacra Captions Contributors. Simulacra aesthetic captions. Technical Report Version 1.0, Stability AI, 2022. url <https://github.com/JD-P/simulacra-aesthetic-captions>. 6
- [37] Alec Radford, Jong Wook Kim, Chris Hallacy, Aditya Ramesh, Gabriel Goh, Sandhini Agarwal, Girish Sastry, Amanda Askell, Pamela Mishkin, Jack Clark, et al. Learning transferable visual models from natural language supervision. In *Int. Conf. Mach. Learn.*, pages 8748–8763. PMLR, 2021. 2, 3
- [38] Jian Ren, Xiaohui Shen, Zhe Lin, Radomir Mech, and David J Foran. Personalized image aesthetics. In *Int. Conf. Comput. Vis.*, pages 638–647, 2017. 1
- [39] Robin Rombach, Andreas Blattmann, Dominik Lorenz, Patrick Esser, and Björn Ommer. High-resolution image synthesis with latent diffusion models. In *IEEE Conf. Comput. Vis. Pattern Recog.*, pages 10684–10695, 2022. 2, 3
- [40] Hamid R Sheikh, Muhammad F Sabir, and Alan C Bovik. A statistical evaluation of recent full reference image quality assessment algorithms. *IEEE Trans. Image Process.*, 15(11):3440–3451, 2006. 6
- [41] Xiangfei Sheng, Leida Li, Pengfei Chen, Jinjian Wu, Weisheng Dong, Yuzhe Yang, Liwu Xu, Yaqian Li, and Guangming Shi. Aesclip: Multi-attribute contrastive learning for image aesthetics assessment. In *ACM Int. Conf. Multimedia*, pages 1117–1126, 2023. 2
- [42] Shaolin Su, Qingsen Yan, Yu Zhu, Cheng Zhang, Xin Ge, Jinqiu Sun, and Yanning Zhang. Blindly assess image quality in the wild guided by a self-adaptive hyper network. In *IEEE Conf. Comput. Vis. Pattern Recog.*, pages 3667–3676, 2020. 2, 7
- [43] Hossein Talebi and Peyman Milanfar. Nima: Neural image assessment. *IEEE Trans. Image Process.*, 27(8):3998–4011, 2018. 1, 2, 7
- [44] Xiaou Tang, Wei Luo, and Xiaogang Wang. Content-based photo quality assessment. *IEEE Trans. Multimedia*, 15(8):1930–1943, 2013. 2
- [45] Unsplash. Access the world’s largest open library dataset, 2023. 8
- [46] Abhinav K Venkataramanan, Cosmin Stejerean, Ioannis Katsavounidis, Hassene Tmar, and Alan C Bovik. Joint quality assessment and example-guided image processing by disentangling picture appearance from content. *arXiv preprint arXiv:2404.13484*, 2024. 3
- [47] Haofan Wang, Matteo Spinelli, Qixun Wang, Xu Bai, Zekui Qin, and Anthony Chen. Instantstyle: Free lunch towards style-preserving in text-to-image generation. *arXiv preprint arXiv:2404.02733*, 2024. 7, 8
- [48] Jianyi Wang, Kelvin CK Chan, and Chen Change Loy. Exploring clip for assessing the look and feel of images. In *Proc. AAAI Conf. Artif. Intell.*, pages 2555–2563, 2023. 2, 4, 5, 7
- [49] Xin Wang, Hong Chen, Zihao Wu, Wenwu Zhu, et al. Disentangled representation learning. *IEEE Trans. Pattern Anal. Mach. Intell.*, 2024. 3
- [50] Yang Wang, Yang Cao, Zheng-Jun Zha, Jing Zhang, Zhiwei Xiong, Wei Zhang, and Feng Wu. Progressive retinex: Mutually reinforced illumination-noise perception network for low-light image enhancement. In *ACM Int. Conf. Multimedia*, pages 2015–2023, 2019. 1
- [51] Haoning Wu, Zicheng Zhang, Erli Zhang, Chaofeng Chen, Liang Liao, Annan Wang, Chunyi Li, Wenxiu Sun, Qiong Yan, Guangtao Zhai, et al. Q-bench: A benchmark for general-purpose foundation models on low-level vision. *arXiv preprint arXiv:2309.14181*, 2023. 4
- [52] Haoning Wu, Zicheng Zhang, Erli Zhang, Chaofeng Chen, Liang Liao, Annan Wang, Kaixin Xu, Chunyi Li, Jingwen Hou, Guangtao Zhai, et al. Q-instruct: Improving low-level visual abilities for multi-modality foundation models. In *IEEE Conf. Comput. Vis. Pattern Recog.*, pages 25490–25500, 2024. 2, 3, 4
- [53] Jiaqi Xu, Mengyang Wu, Xiaowei Hu, Chi-Wing Fu, Qi Dou, and Pheng-Ann Heng. Towards real-world adverse weather image restoration: Enhancing clearness and semantics with vision-language models. In *Eur. Conf. Comput. Vis.*, pages 147–164. Springer, 2024. 4

- [54] Xingqian Xu, Zhangyang Wang, Gong Zhang, Kai Wang, and Humphrey Shi. Versatile diffusion: Text, images and variations all in one diffusion model. In *Int. Conf. Comput. Vis.*, pages 7754–7765, 2023. [7](#), [8](#)
- [55] Yuzhe Yang, Liwu Xu, Leida Li, Nan Qie, Yaqian Li, Peng Zhang, and Yandong Guo. Personalized image aesthetics assessment with rich attributes. In *IEEE Conf. Comput. Vis. Pattern Recog.*, pages 19861–19869, 2022. [6](#), [7](#)
- [56] Zhichao Yang, Leida Li, Yuzhe Yang, Yaqian Li, and Weisi Lin. Multi-level transitional contrast learning for personalized image aesthetics assessment. *IEEE Trans. Multimedia*, 2023. [1](#)
- [57] Zhichao Yang, Leida Li, Pengfei Chen, Jinjian Wu, and Weisheng Dong. Semantics-aware image aesthetics assessment using tag matching and contrastive ranking. In *ACM Int. Conf. Multimedia*, pages 2632–2641, 2024. [2](#), [4](#), [7](#)
- [58] Hu Ye, Jun Zhang, Sibio Liu, Xiao Han, and Wei Yang. Ip-adapter: Text compatible image prompt adapter for text-to-image diffusion models. *arXiv preprint arXiv:2308.06721*, 2023. [3](#), [5](#), [7](#), [8](#)
- [59] Ran Yi, Haoyuan Tian, Zhihao Gu, Yu-Kun Lai, and Paul L Rosin. Towards artistic image aesthetics assessment: a large-scale dataset and a new method. In *IEEE Conf. Comput. Vis. Pattern Recog.*, pages 22388–22397, 2023. [6](#)
- [60] Xin Yuan, Zhe Lin, Jason Kuen, Jianming Zhang, Yilin Wang, Michael Maire, Ajinkya Kale, and Baldo Faieta. Multimodal contrastive training for visual representation learning. In *IEEE Conf. Comput. Vis. Pattern Recog.*, pages 6995–7004, 2021. [2](#)
- [61] Lvmin Zhang, Anyi Rao, and Maneesh Agrawala. Adding conditional control to text-to-image diffusion models. In *Int. Conf. Comput. Vis.*, pages 3836–3847, 2023. [7](#), [8](#)
- [62] Weixia Zhang, Kede Ma, Jia Yan, Dexiang Deng, and Zhou Wang. Blind image quality assessment using a deep bilinear convolutional neural network. *IEEE Trans. Circuit Syst. Video Technol.*, 30(1):36–47, 2020. [2](#), [7](#)
- [63] Weixia Zhang, Guangtao Zhai, Ying Wei, Xiaokang Yang, and Kede Ma. Blind image quality assessment via vision-language correspondence: A multitask learning perspective. In *IEEE Conf. Comput. Vis. Pattern Recog.*, pages 14071–14081, 2023. [1](#), [2](#), [7](#)
- [64] Kai Zhao, Kun Yuan, Ming Sun, Mading Li, and Xing Wen. Quality-aware pre-trained models for blind image quality assessment. In *IEEE Conf. Comput. Vis. Pattern Recog.*, pages 22302–22313, 2023. [3](#)
- [65] Zhipeng Zhong, Fei Zhou, and Guoping Qiu. Aesthetically relevant image captioning. In *Proc. AAAI Conf. Artif. Intell.*, pages 3733–3741, 2023. [4](#)
- [66] Kaiyang Zhou, Jingkang Yang, Chen Change Loy, and Ziwei Liu. Learning to prompt for vision-language models. *Int. J. Comput. Vis.*, 130(9):2337–2348, 2022. [7](#)
- [67] Ye Zhou, Xin Lu, Junping Zhang, and James Z Wang. Joint image and text representation for aesthetics analysis. In *ACM Int. Conf. Multimedia*, pages 262–266, 2016. [3](#), [4](#)
- [68] Hancheng Zhu, Leida Li, Jinjian Wu, Weisheng Dong, and Guangming Shi. Metaiqa: Deep meta-learning for no-reference image quality assessment. In *IEEE Conf. Comput. Vis. Pattern Recog.*, pages 14143–14152, 2020. [1](#), [2](#), [7](#)